Evaluating Receiver Noise Temperature of a Radio Telescope in the Presence of Mutual Coupling: Comparison of Current Methodologies

Daniel Ung[1], Adrian Sutinjo[2], David Davidson[2],
[1]ICRAR - Curtin University, Perth, Australia, daniel.ung@icrar.org
[2]ICRAR - Curtin University, Perth, Australia

***Abstract*—We present the computation of receiver noise temperature which includes the effects of mutual coupling of two different radio telescopes deployed in the Murchison Radio-astronomy Observatory, namely the Murchison Widefield Array and the prototype Engineering Development Array. We used three different formulations that only require information of measured noise parameters of the low noise amplifier as used in the radio telescope and simulated S-parameter of the array to perform the calculation. In addition, we show convergence in computed receiver noise temperature for various pointing angles and array configurations (uniform and pseudo-random) that indicate agreement with existing literature.**

***Index Terms*—Aperture arrays, Radio Telescope, Mutual coupling, Noise receiver temperature, Radio astronomy.**

I. Introduction

Being able to predict the receiver noise temperature of a radio telescope is important for determining the system performance. This information is used to compute the sensitivity (A/T) which is one of the key performance metric given by [1]

$$\frac{A_{\mathrm{e}}}{T_{\mathrm{sys}}} = \frac{A_{\mathrm{e}}}{\eta_{\mathrm{rad}} T_{\mathrm{ext}} + (1-\eta_{\mathrm{rad}})\, T_{\mathrm{a}} + T_{\mathrm{rcv}}} \tag{1}$$

where A_{e} is the effective area, T_{sys} is the system temperature, η_{rad} is the radiation effiency, T_{ext} is the antenna temperature due to sky, T_{a} is the ambient temperature and T_{rcv} is the receiver noise temperature.

In this paper, we are interested in the calculation of the receiver noise temperature. This calculation can be challenging to compute as the complexity increases due to mutual coupling when compared to a single element calculation. While it can be seen in [2], [3] that the receiver noise temperature can be extracted from astronomical observations but it requires that the telescope to be built and fully functional to be able to utilize such techniques. It is preferable to be able to predict receiver noise temperature ahead to time.

As it will be shown in Sect. II, the only information required for such calculation is the measured noise correlation matrix of the low noise amplifier (LNA) and the S-parameter of the array. The formulations used are based on existing literature [4]–[6], which uses different approaches to evaluate the receiver temperature. We will be implementing three separate methods to check the convergence between them.

Following noise extraction of a low noise amplifier (LNA) as utilized by the Murchision Widefield Array (MWA) [7], [8] seen in [9], we now aim to compute the receiver noise temperature of MWA, which is a uniform array, and Engineering Development Array (EDA) [3], which is a pseudo-random array using existing formulations which accounts for mutual coupling.

Section II will briefly touch upon key equations used followed by comparison of results in Section III. Concluding remarks will be presented in Section IV.

II. Existing Methods

A. Method 1

The analysis of total coupled noise waves to the output of the array follows [4]. To illustrate the overall path taken by the noise waves, we use a two-element array as shown in Fig. 1.

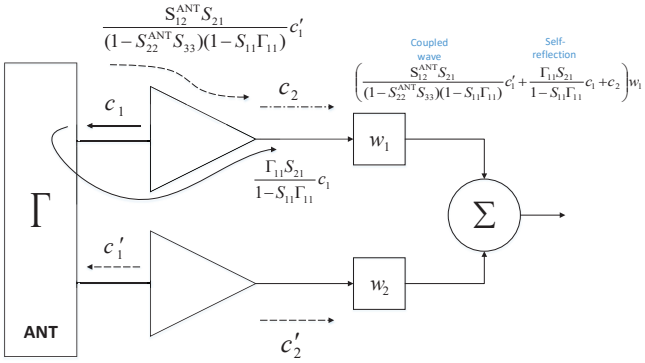

Fig. 1. Coupling path of internal noise sources for a two-element array. The output referred receiver noise temperature consists of reflected wave c_1', coupled wave to neighbouring element c_1' and noise wave c_2 emanating from the output of the receiver. While not shown, similar coupling paths occur at the lower branch.

The total noise power at the output of the summer due to internal sources alone is given by

$$\begin{aligned} P_{\mathrm{int}}^{\mathrm{out}} &= |S_{21}|^2 \langle |c_1|^2 \rangle \mathbf{w} (\mathbf{I} - \mathbf{S}^{\mathrm{ant}} S_{11})^{-1} \\ &\quad \mathbf{S}^{\mathrm{ant}} \left(\mathbf{S}^{\mathrm{ant}}\right)^H (\mathbf{I} - \mathbf{S}^{\mathrm{ant}} S_{11})^{-H} \mathbf{w}^H \\ &\quad + 2\mathbb{R}\{S_{21} \langle c_1 c_2^* \rangle \mathbf{w} (\mathbf{I} - \mathbf{S}^{\mathrm{ant}} S_{11})^{-1} \mathbf{S}^{\mathrm{ant}} \mathbf{w}^H\} \\ &\quad + \langle |c_2|^2 \rangle \mathbf{w} \mathbf{w}^H \end{aligned} \tag{2}$$

where $\mathbf{w} = [w_1 \dots w_n]$ is the complex weighting vector, S_{mn} are the S-parameters of the LNA, $\mathbf{S}^{ant}$ is the S-parameter matrix of the antenna array, $\mathbf{I}$ is an identity matrix, $\langle|c_1|^2\rangle$, $\langle c_1 c_2^*\rangle$ and $\langle|c_2|^2\rangle$ are the noise correlation terms of the LNA. The superscripts $.^H$ and $.^*$ represents the Hermitian and complex conjugate operator respectively.

It can be shown that for a two-element array, (2) produces the exact output power expression seen in Fig. 1. The available gain of an array is given by [4]

$$\begin{aligned} G_A &= \sum_{M}^{m=1} \frac{1-|\zeta\Gamma_{s,m}|^2}{|1-\Gamma_{s,m}S_{11}|^2}|S_{21}w_m|^2|1+\Gamma_{s,m}S_{11}\kappa_m|^2 \\ \zeta &= \frac{1+\kappa_m}{1+\Gamma_{s,m}S_{11}\kappa_m} \\ \Gamma_{s,m} &= \mathrm{row}_m\{(\mathbf{I}-\mathbf{S}^{\mathrm{ant}}\mathbf{S})^{-1}\mathbf{S}_n^{\mathrm{ant}}\} \end{aligned} \tag{3}$$

where $\mathbf{S}_n^{\mathrm{ant}} = [S_{1,n}^{\mathrm{ant}} \dots S_{M,n}^{\mathrm{ant}}]^T$, $\mathbf{S} = S_{11}(\mathbf{I}-\mathbf{J}_{n,n})$ [1] and $\Gamma_{s,m}$ is the reflection coefficient of the embedded element. κ_m is a ratio of the total coupled noise wave at the output of adjacent branches with respect its self-reflected $\langle c_1\rangle$ wave at the output of the m^{th} branch.

B. Method 2

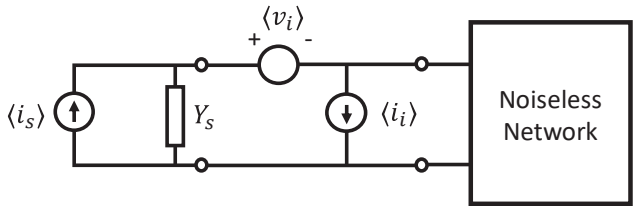

Fig. 2. Circuit representation of input referred voltage and current noise source. The i_s and Y_s are parts of the Norton equivalent circuit of the source attached to the network.

T_{rcv} can be determined by using equivalent voltage and current noise sources using the expression [5]

$$T_{\mathrm{rcv}} = \frac{1}{4k}\frac{\mathbf{wQRQ^Hw^H}}{\mathbf{wQ}\mathbb{R}\{\mathbf{Z}_A\}\mathbf{Q^Hw^H}} \tag{4}$$

$$\mathbf{Q} = Z_{11}\left(Z_{11}\mathbf{I}-\mathbf{Z}_A\right)^{-1} \tag{5}$$

$$\mathbf{R} = \mathbf{V}_{n,R}^2 + \mathbf{Z}_A\mathbf{Y}_c\mathbf{V}_{n,R}^2 + \mathbf{V}_{n,R}^2\mathbf{Y}_c^H\mathbf{Z}_A^H + \mathbf{Z}_A\mathbf{I}_{n,R}^2\mathbf{Z}_A^H \tag{6}$$

where Z_{11} is the input impedance of the LNA, $\mathbf{Z}_A$ is the impedance matrix of the mutually coupled elements, $\mathbf{V}_{n,R}^2$, $\mathbf{I}_{n,R}^2$ and $\mathbf{Y}_c$ are diagonal matrices of squared noise voltage densities, squared noise current densities and correlation admittance of the LNA.

The noise parameters of the LNA can be converted into an input referred noise voltage and current sources as shown in Fig. 2 and the relationship between the two can be found in [10].

[1] $\mathbf{J_{n,n}}$ represents a single-entry matrix at row n, column n

C. Method 3

Using a more general multiport approach found in [6] we can compute the outgoing receiver noise power (see Fig. 1) using

$$\mathbf{P}_{\mathrm{int}}^{\mathrm{out}} = \mathbf{wM\hat{N}M}^H\mathbf{w}^H \tag{7}$$

$$\mathbf{M} = \left[1-\mathbf{S}^{\mathrm{LNA}}\mathbf{S}^{\mathrm{load}}\right]^{-1} \tag{8}$$

where $\mathbf{P}_{\mathrm{int}}^{\mathrm{out}}$ is a matrix containing the outgoing noise power at each port, $\hat{\mathbf{N}}$ is the noise correlation matrix of the multiport amplifier, $\mathbf{M}$ accounts for the mismatches in impedance, $\mathbf{S}^{\mathrm{LNA}}$ is the S-parameters of the multiport amplifier and $\mathbf{S}^{\mathrm{load}}$ is the S-parameters of the combined source and load network attached to the multiport amplifier.

The contribution of external noise is calculated using

$$\mathbf{P}_{\mathrm{ext}}^{\mathrm{out}} = \mathbf{wMS}^{\mathrm{LNA}}\mathbf{A}\left(\mathbf{S}^{\mathrm{LNA}}\right)^H\mathbf{M}^H\mathbf{w}^H \tag{9}$$

$$\tag{10}$$

where $\mathbf{A}$ contains the incident noise correlation matrix due to external sources.

Finally, the receiver noise temperature is given by

$$T_{\mathrm{rcv}} = \frac{\mathbf{P}_{\mathrm{int}}^{\mathrm{out}}}{\mathbf{P}_{\mathrm{ext}}^{\mathrm{out}}}T_0 \tag{11}$$

III. Results

We simulated an MWA tile (16 element) and the 256 element array (EDA) using an electromagnetic simulation package called FEKO to obtain the S-parameter of the array. We then apply the various T_{rcv} formulations presented in Sect. II using the measured noise parameters and S-parameters of the LNA previously measured in [9].

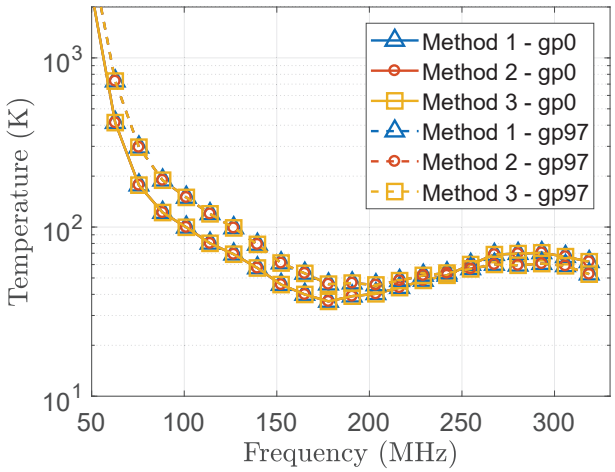

Fig. 3. Comparison of MWA receiver noise temperatures computed using various methods over two separate pointing. The legend gp0 and gp97 represents a pointing direction of $\phi = 90°$, $\theta = 0°$ and $\phi = 45°$, $\theta = 42°$ respectively.

Fig. 3 and 4 shows the calculated receiver noise temperature using three different methods of the MWA and EDA. We

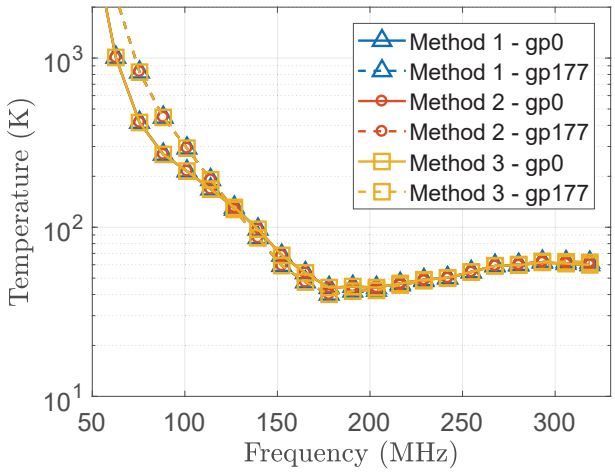

Fig. 4. Comparison of EDA receiver noise temperatures computed using various methods over two separate pointing. The legend gp177 represents a pointing direction of $\phi = 66.8°$, $\theta = 64.5°$.

note that all three different methods presented converges for various pointing direction and array configurations (uniform and pseudo-random configuration) which indicated agreement in current literature of computing receiver noise temperature.

IV. Conclusion

We demonstrated the ability to compute the receiver noise temperature of MWA and EDA based on the simulated S-parameter of the array and measured noise parameters of an MWA LNA at various pointing angle. In addition, we showed that the three different formulations found in current literature for computing receiver noise temperature converges.

Based on the work presented, we showed that receiver noise temperature of a radio telescope can be computed ahead of time without requiring the array to be built and can be used for characterizing future generation telescopes such as the Square Kilometre Array (SKA) [11].

References

[1] K. F. Warnick, M. V. Ivashina, R. Maaskant, and B. Woestenburg, "Unified definitions of efficiencies and system noise temperature for receiving antenna arrays," *IEEE Transactions on Antennas and Propagation*, vol. 58, no. 6, pp. 2121–2125, June 2010.

[2] J. D. Bowman, D. G. Barnes, F. H. Briggs, B. E. Corey, M. J. Lynch, N. D. R. Bhat, R. J. Cappallo, S. S. Doeleman, B. J. Fanous, D. Herne, J. N. Hewitt, C. Johnston, J. C. Kasper, J. Kocz, E. Kratzenberg, C. J. Lonsdale, M. F. Morales, D. Oberoi, J. E. Salah, B. Stansby, J. Stevens, G. Torr, R. Wayth, R. L. Webster, and J. S. B. Wyithe, "Field Deployment of Prototype Antenna Tiles for the Mileura Widefield Array Low Frequency Demonstrator," *AJ*, vol. 133, pp. 1505–1518, Apr. 2007.

[3] R. Wayth, M. Sokolowski, T. Booler, B. Crosse, D. Emrich, R. Grootjans, P. J. Hall, L. Horsley, B. Juswardy, D. Kenney, K. Steele, A. Sutinjo, S. J. Tingay, D. Ung, M. Walker, A. Williams, A. Beardsley, T. M. O. Franzen, M. Johnston-Hollitt, D. L. Kaplan, M. F. Morales, D. Pallot, C. M. Trott, and C. Wu, "The Engineering Development Array: A Low Frequency Radio Telescope Utilising SKA Precursor Technology," *PASA*, vol. 34, p. e034, Aug. 2017.

[4] L. Belostotski, B. Veidt, K. F. Warnick, and A. Madanayake, "Low-noise amplifier design considerations for use in antenna arrays," *IEEE Transactions on Antennas and Propagation*, vol. 63, no. 6, pp. 2508–2520, June 2015.

[5] K. F. Warnick, B. Woestenburg, L. Belostotski, and P. Russer, "Minimizing the noise penalty due to mutual coupling for a receiving array," *IEEE Transactions on Antennas and Propagation*, vol. 57, no. 6, pp. 1634–1644, June 2009.

[6] J. Randa, "Noise characterization of multiport amplifiers," *IEEE Transactions on Microwave Theory and Techniques*, vol. 49, no. 10, pp. 1757–1763, Oct 2001.

[7] S. J. Tingay, R. Goeke, J. D. Bowman, D. Emrich, S. M. Ord, D. A. Mitchell, M. F. Morales, T. Booler, B. Crosse, R. B. Wayth, C. J. Lonsdale, S. Tremblay, D. Pallot, T. Colegate, A. Wicenec, N. Kudryavtseva, W. Arcus, D. Barnes, G. Bernardi, F. Briggs, S. Burns, J. D. Bunton, R. J. Cappallo, B. E. Corey, A. Deshpande, L. Desouza, B. M. Gaensler, L. J. Greenhill, P. J. Hall, B. J. Hazelton, D. Herne, J. N. Hewitt, M. Johnston-Hollitt, D. L. Kaplan, J. C. Kasper, B. B. Kincaid, R. Koenig, E. Kratzenberg, M. J. Lynch, B. Mckinley, S. R. Mcwhirter, E. Morgan, D. Oberoi, J. Pathikulangara, T. Prabu, R. A. Remillard, A. E. E. Rogers, A. Roshi, J. E. Salah, R. J. Sault, N. Udaya-Shankar, F. Schlagenhaufer, K. S. Srivani, J. Stevens, R. Subrahmanyan, M. Waterson, R. L. Webster, A. R. Whitney, A. Williams, C. L. Williams, and J. S. B. Wyithe, "The Murchison Widefield Array: The Square Kilometre Array Precursor at Low Radio Frequencies," *PASA*, vol. 30, p. e007, Jan. 2013.

[8] R. B. Wayth, S. J. Tingay, C. M. Trott, D. Emrich, M. Johnston-Hollitt, B. McKinley, B. M. Gaensler, A. P. Beardsley, T. Booler, B. Crosse, T. M. O. Franzen, L. Horsley, D. L. Kaplan, D. Kenney, M. F. Morales, D. Pallot, G. Sleap, K. Steele, M. Walker, A. Williams, C. Wu, I. H. Cairns, M. D. Filipovic, S. Johnston, T. Murphy, P. Quinn, L. Staveley-Smith, R. Webster, and J. S. B. Wyithe, "The Phase II Murchison Widefield Array: Design overview," *PASA*, vol. 35, Nov. 2018.

[9] A. T. Sutinjo, D. C. X. Ung, and B. Juswardy, "Cold-source noise measurement of a differential input single-ended output low-noise amplifier connected to a low-frequency radio astronomy antenna," *IEEE Transactions on Antennas and Propagation*, vol. 66, no. 10, pp. 5511–5520, Oct 2018.

[10] H. A. Haus, W. R. Atkinson, G. M. Branch, W. B. Davenport, W. H. Fonger, W. A. Harris, S. W. Harrison, W. W. Mcleod, E. K. Stodola, and T. E. Talpey, "Representation of noise in linear twoports," *Proceedings of the IRE*, vol. 48, no. 1, pp. 69–74, Jan 1960.

[11] P. E. Dewdney, P. J. Hall, R. T. Schilizzi, and T. J. L. W. Lazio, "The Square Kilometre Array," *IEEE Proceedings*, vol. 97, pp. 1482–1496, Aug. 2009.